

## Characterization of Alpha Bismuth Trioxide Nanoparticles and their Application for Catalytic Degradation of Xylene Cyanol FF Dye in Aqueous Solution

<sup>1</sup>F. Akbar Jan\*, <sup>1</sup>Rahat Ullah, <sup>1</sup>Umar Shah, <sup>1</sup>Muhammad Saleem, <sup>2</sup>Naimat Ullah, <sup>3</sup>Muhammad Usman

<sup>1</sup>Department of Chemistry, Bacha Khan University Chrasadda, Khyber-Pakhtunkhwa, 24420 Pakistan.

<sup>2</sup>Department of Chemistry, Quaid-i- Azam University Islamabad, 45320 Pakistan.

<sup>3</sup>Center for Research Excellence in Nanotechnology, King Fahd University of Petroleum and Minerals, Dhahran 31261, Saudi Arabia.

[fazal\\_akbarchem@yahoo.com\\*](mailto:fazal_akbarchem@yahoo.com)

(Received on 10<sup>th</sup> September 2020, accepted in revised form 27<sup>th</sup> January 2021)

**Summary:** Bismuth oxide (Bi<sub>2</sub>O<sub>3</sub>) nanoparticles were synthesized using chemical reduction method. The prepared nanoparticles were characterized by Ultra violet – Visible (UV-Vis) spectroscopy, X-ray diffraction (XRD), Fourier Transform Infra-red (FTIR) spectroscopy, Scanning electron microscopy (SEM) and Energy dispersive X-ray (EDX) techniques. The characterized nanoparticles were applied as photo catalyst for the degradation of hazardous dye Xylene Cyanol FF in aqueous medium. The effects of different parameters such as irradiation time, initial dye concentration, catalyst dosage, pH of the medium and temperature were studied on the photo catalytic degradation of the dye. It was found that with increase in irradiation time and catalyst dosage the degradation exponentially increased and decreased with increase in initial concentration of the dye. The temperature was found to have no appreciable effect on the dye degradation in open atmosphere.

**Keywords:** Bismuth oxide nanoparticles; Xylene Cyanol FF dye, Band gap; Photo catalytic activity.

### Introduction

Water pollution caused due to industrialization, growing population, and consumerism has become a severe environmental issue in recent years [1]. Textile and dyeing industries are among the major identified sources of pollution of surface and underground water. A number of organic compounds are present in the drainage of these industries. Adsorption, biological treatment and coagulation like conventional water treatment methods cannot degrade these chemicals. [2]. About 10,000 tons of dyes are produced per year according to the literature. Approximately 12 % of used dyes is lost during manufacturing and processing operations. The dyes are the most important constituent of emulsifiers, cosmetics, viscosity enhancing agents, stabilizers, antioxidants, lubricating substances and moisturizing agents [3, 4]. Among the health hazards caused due to dye exposure or inhalation the respiratory problems, immune system problems, watery eyes, sneezing, asthma and wheezing are more common [5]. Free aromatic amines have been found to be formed from the ingested dyes during metabolism at the intestinal wall and in the liver that are potentially carcinogenic and mutagenic [6]. Chromosomal aberration in mammalian cells and bladder cancer in humans is caused by many azo group containing dyes. [7]. Contact dermatitis also develops from exposure to ultraviolet light when these substances on the skin associated with skin proteins modify. One of the most commonly used dyes is Xylene cyanol FF which is

used in textile industry and also as a laboratory substance for the determination of amines, trace nitrite and aniline. The leuco form (LXCFF) of this dye is also used for the determination of trace quantity of gold, Cr(VI), iron and aluminum in ores, rock and minerals [8,9]. Electron rich oxygen group ( $-\text{SO}^{-3}$ ) is present in its structure. These negatively charged  $-\text{SO}^{-3}$  groups on the electrode surface have a high affinity towards the positively charged analyte in the solution and produce high current signals with L-dopa [10-12]. Owing to high operating cost and production of large volume of sludge conventional waste water treatment methods are ineffective. Due to economy, cheapness, environmental friendly and production of no or less toxic byproducts the photo catalysis is now a days a potential method for environmental clean-up [13,14]. For the last two decades due to their unusual physical properties nano structured materials have turned the attention of the scientific, academic, and industrial communities. Bismuth (Bi) oxides and sulphides have high Hall coefficient, low thermal conductivity and high electrical resistivity. Because of their efficient photo catalytic performance, low toxicity, high stability and cost-effectiveness bismuth-related nanoparticles including Bi<sub>2</sub>WO<sub>6</sub>, BiOCOOH, BiVO<sub>4</sub>, BiPO<sub>4</sub>, (BiO)<sub>2</sub>CO<sub>3</sub>, BiOCl and Bi<sub>2</sub>O<sub>3</sub> have gained considerable importance. Bismuth oxide being p-type semi conductor material are widely used in the field of catalysis, photoelectric materials, high temperature superconductor materials, solid oxide

---

\*To whom all correspondence should be addressed.

fuel cells, gas sensors and functional ceramics.  $\text{Bi}_2\text{O}_3$  has five major polymorphic forms that are denoted as  $\alpha$ -,  $\beta$ -,  $\gamma$ -,  $\delta$ - and  $\omega$ -  $\text{Bi}_2\text{O}_3$  [15,16]. Keeping in view the benefits of the photo catalysis it offers over the other conventional treatments methods a study was designed to synthesize and characterize the bismuth oxide  $\alpha$ - $\text{Bi}_2\text{O}_3$  nanoparticles and to use as a catalyst for the photo degradation of Xylene Cyanol FF dye in aqueous medium.

## Experimental

### Reagents and Instruments

Analytical grade reagents such as bismuth nitrate penta hydrate, nitric acid, ammonium hydroxide and Xylene cyanol FF dye were purchased from Sigma Aldrich.

UV-visible spectrophotometer Model Shimadzu UV-1800, Japan was used for all absorbance measurements. Perkin Elmer FTIR spectrometer version 10.4.00 was used for identification of the functional groups. Elico (model IL-610) digital pH meter was used for pH measurements. All the analysis was performed in Advance Research Lab (ARL) Department of Chemistry Bacha Khan University Charsadda. XRD, SEM and EDX analysis of the synthesized materials were carried out in the Center for Research Excellence in Nanotechnology, King Fahd University of Petroleum and Minerals, Dhahran Saudi Arabia.

### Preparation of Bi-oxide nanoparticles

$\alpha$ - $\text{Bi}_2\text{O}_3$  nanoparticles were synthesized using chemical reduction method. In the synthesis method 2 g of bismuth nitrate penta hydrate was dissolved in 0.1 N Nitric acid ( $\text{HNO}_3$ ). Side wise 0.5 M aqueous solution of Ammonium hydroxide was also prepared. The homogenous solution of Bismuth nitrate was kept on the preheated oil bath on the hot plate. Large size thermometer was dipped in the oil bath to note the temperature of the solution. When the temperature was reached 80 °C Ammonium hydroxide solution was added drop wise with constant stirring until the pH reached 9. The yellow color solution formed was stirred for 3 hr. The resultant suspension was cooled to room temperature followed by filtration and washing 5 times with distilled water in order to neutralize pH. The filtrates

were oven dried for 2 hr at 90°C and then calcined in muffle furnace for 2 hr at 400 °C. The nanoparticles were stored in air tight vials for further experiments.

### Preparation of dye solution

Stock solution (500ppm) of Xylene Cyanol FF was prepared by dissolving 0.125 gram of dye in distilled water. Then working solutions of different concentrations were prepared using the following dilution formula (Eq.1)

$$C_1V_1=C_2V_2 \quad (1)$$

### Photo catalytic activity

Photo catalytic activity of  $\alpha$ - $\text{Bi}_2\text{O}_3$  was evaluated while using it for the photo degradation of Xylene Cyanol FF dye under UV light. Initially 500 ppm solution of Xylene Cyanol FF was prepared which was used for further activities. The wavelength of maximum absorption of the dye was found that was 614 nm using UV-visible spectrophotometer. Bismuth oxide was added to the working solution. The suspension before exposure to light source was stirred for 20 minutes till adsorption desorption equilibrium.

## Results and Discussion

### Characterization of the $\alpha$ - $\text{Bi}_2\text{O}_3$ nanoparticles

#### UV-Vis spectroscopy

The UV-Visible spectrum of Bismuth oxide ( $\alpha$   $\text{Bi}_2\text{O}_3$ ) nanoparticles is shown in Fig. 1a. The spectrum shows characteristic absorption at wavelengths of 415 nm [17].

Using equation (2) the band gap was calculated from UV-Visible spectrum.

$$\alpha h\nu = A(h\nu - E_g)^n \quad (2)$$

Absorption coefficient is represented by  $\alpha$ , energy of photon by  $h\nu$  and proportionality constant by  $A$  respectively. From the graph the optical band gap of Bismuth oxide nanoparticles was calculated, which came out to be 2.5 eV as shown in Fig.-1b. It is closely related to literature value [18].

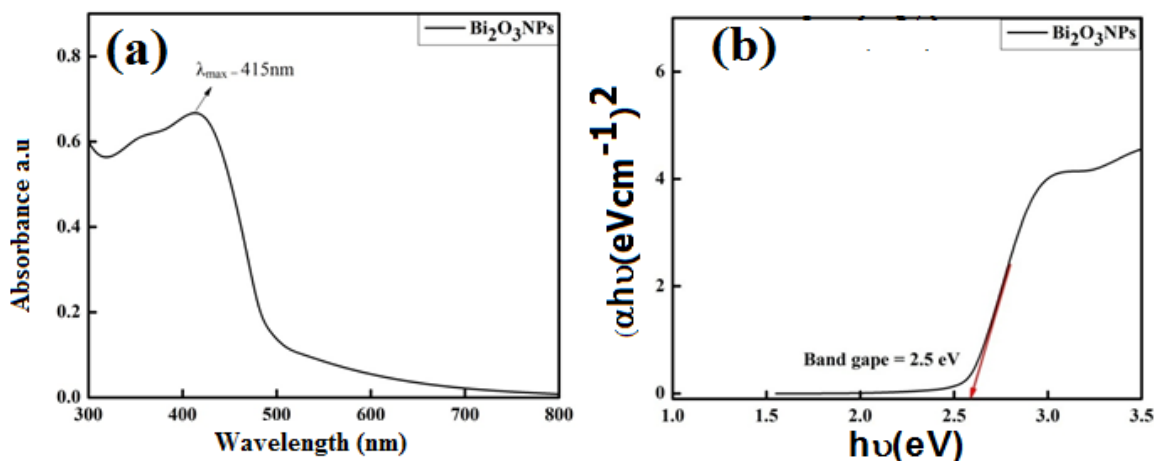


Fig. 1: (a) UV-Visible spectrum of Bismuth oxide ( $\alpha$   $\text{Bi}_2\text{O}_3$ ) nanoparticles. (b) band gap of Bismuth oxide ( $\alpha$   $\text{Bi}_2\text{O}_3$ ) nanoparticles.

#### XRD Studies

The XRD patterns of  $\alpha$ - $\text{Bi}_2\text{O}_3$  nanoparticles are shown in Figure 2. This pattern shows monoclinic system with concerned peaks and indexed is according to the JCPDS card number 41-1449. The observed results of  $\alpha$ - $\text{Bi}_2\text{O}_3$  NPs reveal the linear parameters of  $a = 5.8499$ ,  $b = 8.1698$  and  $c = 7.5123$ . Additionally the angular parameters are  $\alpha = 90^\circ$ ,  $\beta = 112.988^\circ$  and  $\gamma = 90^\circ$  respectively. The corresponding peaks are closely related to literature [19].

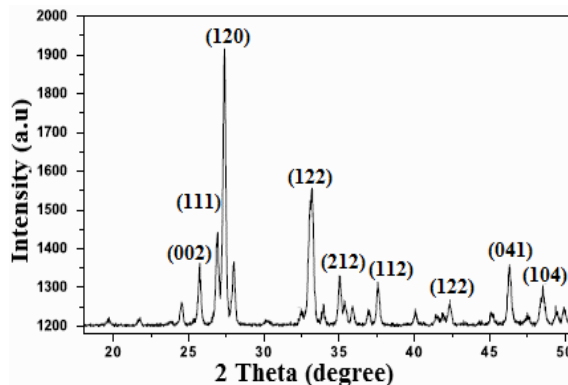


Fig. 2: XRD pattern of  $\alpha$ - $\text{Bi}_2\text{O}_3$  nanoparticles.

By using the XRD data the average crystallite size of  $\alpha$ - $\text{Bi}_2\text{O}_3$  NPs was calculated with the help of Debye-Scherrer equation (Eq.3).

$$D = \frac{K\lambda}{\beta \cos\theta} \quad (3)$$

where "K" is constant with a value of 0.9, wavelength of X-rays is represented by  $\lambda$ , Full width half maxima by  $\beta$  is and Bragg diffraction angle of the concerned peak by  $\theta$  respectively. The average crystallite size value comes out to be 24.34 nm.

#### SEM with EDX analysis

The SEM image given in Fig.3a shows that the  $\alpha$ - $\text{Bi}_2\text{O}_3$  calcined powders are composed of large scale uniform solid  $\text{Bi}_2\text{O}_3$  particles that correspond to the alpha phase of the oxide and have a random orientation [20,21]. Recorded image showed that the synthesized  $\text{Bi}_2\text{O}_3$  nano particles are compact structure with spiky ends[22]. EDX analysis was perform for the investigation of elemental purity of the prepared nanoparticles (Fig.3b, Table 1). The results showed the presence of Bi and O only. Peaks of any other elements are absent. This confirmed the elemental purity of  $\text{Bi}_2\text{O}_3$  and is free of other elements [23].

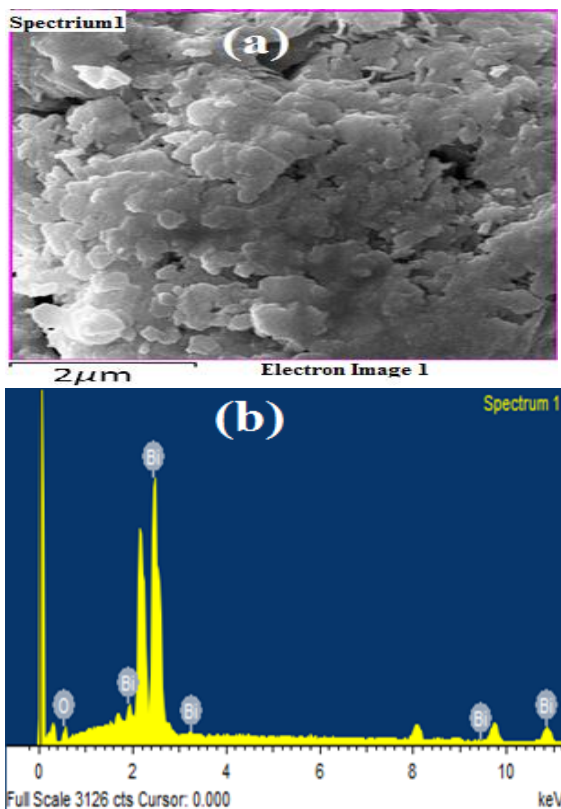


Fig. 3: (a) SEM image of Bi-oxide nanoparticles (b) EDX image of Bi-oxide nanoparticles.

#### FTIR analysis

The FTIR spectrum is given in Fig. 4. A band at  $454.2\text{ cm}^{-1}$  could be the characteristics vibrations of Bi-O bond. Sharp band at  $1391\text{ cm}^{-1}$  is due to the presence of  $\text{NO}_3^-$  group [24]. The absorption band at  $829\text{ cm}^{-1}$  and  $1034\text{ cm}^{-1}$  shows C-O stretching and  $\alpha\text{-Bi}_2\text{O}_3$  crystalline Bi-O modes respectively which are the characteristic of  $\alpha\text{-Bi}_2\text{O}_3$  [25, 26].

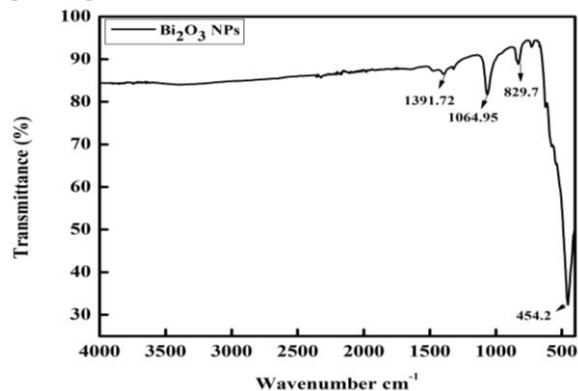


Fig. 4: FTIR spectrum of  $\alpha\text{-Bi}_2\text{O}_3$  nanoparticles.

Table-1: Elemental composition of Bi-oxide nanoparticles.

Element	Weight%	Atomic%
O	8.86	O
Bi	91.14	Bi
Totals	100.00	Totals

#### Photocatalytic degradation of Xylene Cyanol FF dye

The photo degradation of Xylene Cyanol FF in aqueous medium in the presence of atmospheric air using  $\text{Bi}_2\text{O}_3$  as photo catalysts was studied carrying out the reaction under UV lamps. A known quantity of the catalyst was added and the suspension was kept under the UV lamp. Initially the dye solution was dark blue in color, after the photo degradation the color of the solution changed to light blue. About 5 ml of the reaction mixture was taken out at different intervals and centrifuged for 10 minutes and analyzed by UV-visible spectrophotometer to study the degradation rate. The percent degradation was calculated using following relation (Eq.4).

$$(A_o - A_t / A_o) \times 100 \quad (4)$$

where  $A_o$  shows the absorbance at time  $t = 0$  and  $A_t$  is the absorbance at  $t = t$ .  $A_o$  and  $A_t$  are recorded at  $\lambda_{\text{max}}$  of dye.

#### Effect of irradiation time on dye degradation

First 5 ml of the original Xylene Cyanol FF solution was taken and the maximum absorption was noted that was 614 nm. For studying the photo degradation of dye, 50 ml solution was taken and 0.02 g of proposed photo catalyst was added and kept in dark with the continuous stirring in order to ensure adsorption and desorption equilibrium. For time duration of 10 minutes to 150 minutes the suspension was irradiated with UV light. Initially the degradation was 4.29% at 10 minutes interval then raised to 59% at 150 minutes. Time interval of 150 minutes was recorded as optimum time for the degradation of the dye. Fig.5 shows the effect of time on the dye degradation. Previous study [27] has reported the photo catalytic degradation of Methylene blue and Methyl orange using  $\alpha\text{-Bi}_2\text{O}_3$  nanoparticles. They have reported 77 % and 76 % degradation under light irradiation at 240 minutes time duration for Methyl orange and Methylene blue respectively.

Enhancement of the degradation with time can be attributed to the fact that on the surface of catalyst more dye molecules adsorbs as well as the production of  $\text{OH}^\bullet$  needed for the dye molecules

increases on exposure to UV light which accounts for the photocatalyst activity.

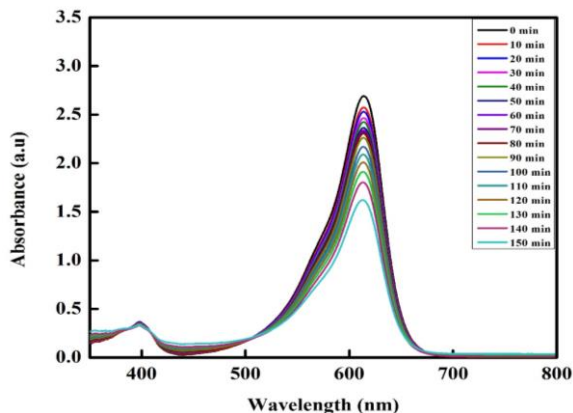


Fig. 5: Effect of irradiation time on dye degradation.

#### Effect of initial concentration on dye degradation

On the dye degradation the effect of initial concentration was studied using different concentrations varying from 10 ppm to 70 ppm keeping all other factors identical. The percent degradation in the low dye concentration (10 ppm) was observed to be 59% and then decreased up to 1.2% when the dye concentration was increased. On the catalyst surface more dye molecules adsorbed claiming degradation. Keeping catalyst dose constant and increasing the concentration of dye, catalyst surface gets saturated. Simultaneously intense color of dye does not permit light to reach photo catalyst. Fig. 6. depicts the effect of initial dye concentration on degradation.

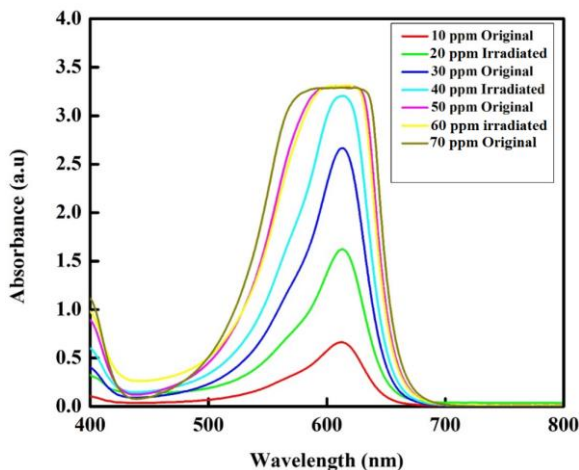


Fig. 6: Effect of concentration on dye degradation.

#### Effect of dosage rate on the dye degradation

Another factor that affects the rate of degradation is the catalyst dose. Catalyst weight up to certain extent increases the degradation and above this the rate of degradation of the dye decreases with increase in weight. Exposed surface area of the catalyst is the factor on which photo degradation depends upon and the availability of exposed surface area of the catalyst will not be in direct relation to the amount of catalyst added in solution phase reactions. When the dye molecules adsorb on the catalyst surface a saturation point is reached beyond which the catalyst amount may not have a direct relationship to the degradation extent. Most of the studies have revealed that 3-4 g per liter of the solid is required for maximum activity [28]. The process was performed by the addition of various amount of catalyst keeping the concentration of dye and time of irradiation constant. The catalyst dose was increased from 0.01 to 0.04 g. Maximum degradation was noticed in case of catalyst dose of 0.02 g that was 70% beyond which the percent degradation decreases exponentially as shown in the Fig. 7. This can be attributed to the shielding of the photons by the suspension [29, 30].

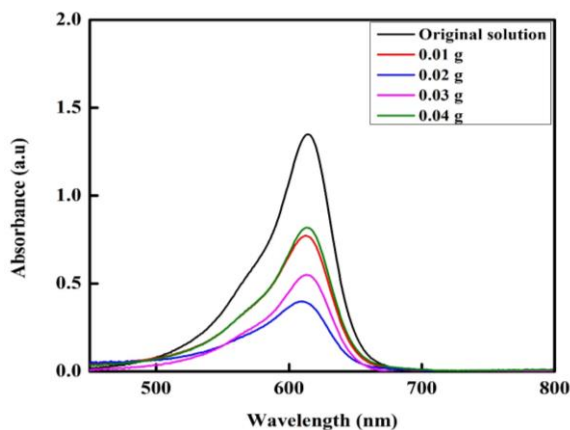


Fig. 7: Effect of dosage rate on dye degradation.

#### Effect of pH on the dye degradation

Dye degradation also depends on the pH of the solution. The pH of the solution of Xylene Cyanol FF was checked by pH meter. The pH of Xylene Cyanol FF was 6.39 which were slightly acidic this is why it is also called Acid blue 147 [31]. For pH study 20 ppm solution was prepared in 250 ml of the distilled water. Then solutions of different pH were prepared by adding 0.1 N HCl and 0.1 N NaOH solutions. The pH of the solutions was kept from 5 to 8 and 0.02 gram of the amount of the

catalyst was added each. At pH 5 high degradation was recorded that was 99%. Increasing the pH of the solution the degradation decreased as at pH 6 the degradation was only 47% and then 27% and 19% respectively at higher pH. The effect of pH on degradation is shown in Fig.8. For the photocatalytic degradation process, adsorption of dye is an essential step. Faster the dye will degrade which have high adsorption capacity. Higher concentration of hydroxyl ions is provided at higher pH to react with holes on the semiconductor materials forming OH radicals which subsequently causes an improved photocatalytic degradation of dyes. The extent of degradation is determined by the concentration of hydroxyl radicals and adsorption on photocatalyst [32]. The potential of the surface charge in photocatalyst/aqueous systems is determined by the activity of ions (e.g. H<sup>+</sup> or pH). pH affects the property of a surface to become either positively or negatively charged [29, 30].

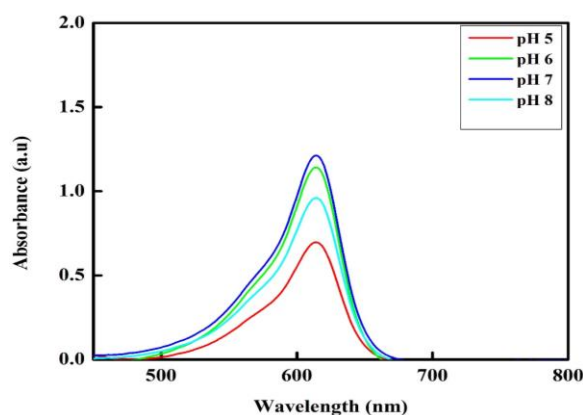


Fig.8: (a) Effect of pH of the medium on dye degradation (b) Effect of Temperature on the dye degradation.

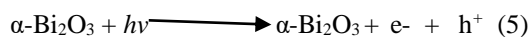
#### Effect of temperature on degradation

The temperature of the medium also has an immense effect on the degradation of the dye. In order to know about the effect of the temperature on the dye degradation a solution of 10 ppm was prepared and then 50 ml from the stock solution was kept with the addition of 0.02 gram of  $\alpha$ -Bi<sub>2</sub>O<sub>3</sub> nanoparticles under the UV for different time periods from 40 to 150 minutes. At the temperature of 20°C, 30°C, 40°C and 50°C the samples were taken out and analyzed. The maximum degradation was recorded at the temperature of 20°C which was about 60% while the degradation at 30°C, 40°C and 50°C was not appreciable. The percent degradation in open beakers decreased with the increase in temperature due to

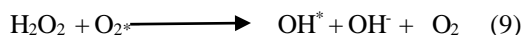
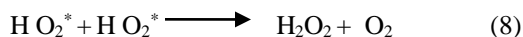
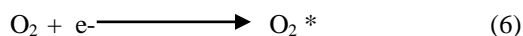
the evaporation of the solvent. When the temperature of reaction is below 80 °C it favors the adsorption when it further reduces to 0 °C there is increase in the noticeable activation energy occurs [33, 34]. The desired temperature for the effective photo mineralization of organic content is temperature range between 20-80 °C.

#### Mechanism of photocatalytic activity of $\alpha$ -Bi<sub>2</sub>O<sub>3</sub>

When semiconducting nanoparticles are added to light irradiation this causes accelerated chemical reactions which result in the formation of free radical species [O<sup>-</sup> and OH\*] which degrade organic pollutants (dyes). Under UV light irradiation photocatalytic reaction takes place on the surface of  $\alpha$ -Bi<sub>2</sub>O<sub>3</sub> nanoparticles. The calculated band gap of synthesized  $\alpha$ -Bi<sub>2</sub>O<sub>3</sub> NPs is 2.8 eV and thus easily be activated by UV radiations. Upon UV light irradiation the electrons in the valence band (VB) get excited to conduction band (CB), leaving the holes in the VB of the  $\alpha$ -Bi<sub>2</sub>O<sub>3</sub> photocatalyst as in equation (5) and Fig. 9.



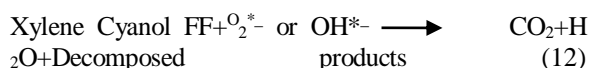
The electron-hole pairs thus generated act as oxidizing and reducing agents. Oxygen acts as an electron acceptor which then reacts with photo-generated electrons at the surface of  $\alpha$ -Bi<sub>2</sub>O<sub>3</sub> as indicated by equation (6)



The produced holes have electrons accepting tendency and act as very strong oxidizing agents. Once migrated to the surface of the  $\alpha$ -Bi<sub>2</sub>O<sub>3</sub> nanoparticles adsorbed water molecule or hydroxide ion is oxidized to form hydroxyl radicals according to equation (10).



Since, the overall photocatalytic degradation mechanism of Xylene Cyanol FF can be represented as in equation (12)



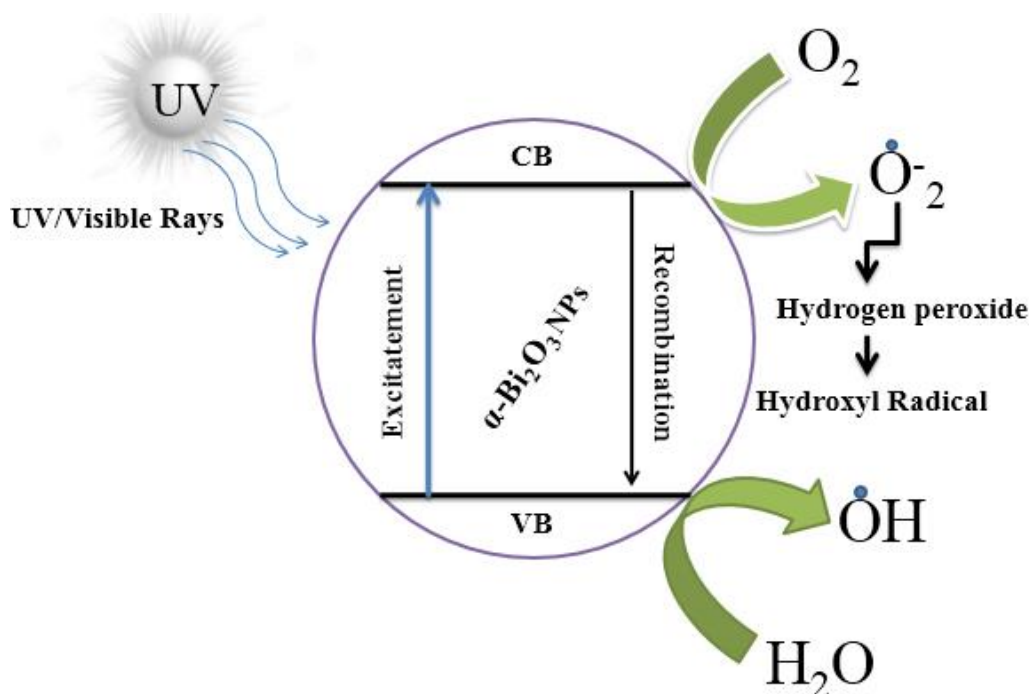


Fig. 9: Mechanism of photocatalytic activity of  $\text{Bi}_2\text{O}_3$ .

### Conclusions

It can be concluded that the synthesized  $\alpha\text{-Bi}_2\text{O}_3$  nanoparticles showed good photocatalytic activity in the degradation of Xylene Cyanol FF dye in aqueous solution. Increase in irradiation time exponentially increased the degradation rate. The concentration has inverse relation with the degradation of the dye. Time duration of 150 minutes and pH 5 was found optimum time and pH for the degradation of the given dye. The degradation increase with dosage rate up to some extent while decrease above that. The temperature has no appreciable role in the photocatalytic degradation of dye in open atmosphere. So it is suggested that degradation of Xylene cyanol FF dye must be carried out in close system.

### References

1. A. Minelgite, G. Liobikiene, The problem of not waste sorting behavior, Comparison of waste sorters and non-sorters in European Union: Cross-cultural analysis, *Sci. Total Environ.*, **672**, 174 (2019).
2. S. Gita, A. Hussain, T. G. Choudry, Impact of textile dyes waste on aquatic environments and its treatment, *Environ. Ecol.*, **35**, 2349 (2017).
3. W. A. Żukiewicz-sobczak, P. Adamczuk, P. Wroblewska, J. Zwolinski, J. Chmielewska-badora, E. Krasowska, J. Kozlik, Allergy to selected cosmetic ingredients, *Adv. Dermat. Aller./Postepy Dermatologii i Alergologii*, **30**, 307 (2013).
4. J. Sima, P. Hasal Photocatalytic degradation of textile dyes in a  $\text{TiO}_2/\text{UV}$  System, *Chem. Eng.*, **32**, 79-84 (2013).
5. M. A. Hassan, A. El Nemr, F. F. Madkour, Environmental assessment of heavy metal pollution and human health risk, *Am. J. Water Sci. Eng.*, **2**, (2016).
6. F. Akarsalan, H. Demiralay, Effects of textile materials harmful to human health, *Acta. Physica Polonica, A*, **128**, B-407 (2015).
7. Ratna, B. S. Padhi, Pollution due to synthetic dyes toxicity & carcinogenicity studies and remediation, *Inter. J Environ. Sci.*, **3**, 940 (2012).
8. H. D. Revanasiddappa, T. K. Kumar, A highly sensitive spectrophotometric determination of chromium using leuco Xylene cyanol FF, *Talanta*, **60**, 1 (2003).
9. L. Cai, C. Xu, Determination of iron and aluminum based on the catalytic effect on the reaction of xylene cyanol FF with hydrogen peroxide and potassium periodate, *J. Braz. Chem. Soc.*, **22**, 1987 (1987).
10. M. Pandurangachar, B. K. Swamy, U. Chandra, O. Gilbert, B. S. Sherigara, Simultaneous determination of dopamine, ascorbic acid and uric acid at poly (Patton and Reeder's) modified carbon paste electrode, *Inter. J Electrochem. Sci.*, **4**, 672 (2009).

11. H. Yao, Y. Sun, X. Lin, Y. Tang, L. Huang, Electrochemical characterization of poly (eriochrome black T) modified glassy carbon electrode and its application to simultaneous determination of dopamine, ascorbic acid and uric acid, *Electrochim. Acta*, **52**, 6165 (2007).
12. S. S.Shankar, B. K.Swamy, B. N.Chandrashekar, K. J.Gururaj, Sodium do- decyl benzene sulfate modified carbon paste electrode as an electrochemical sensor for the simultaneous analysis of dopamine, ascorbic acid and uric acid: A voltammetric study, *J Mol. Liq.*, **177**, 32 (2013).
13. Anku, W. Williumar, K. S.Sudheesh, P. G. Poomani, Graft Gum Ghatti Caped Cu<sub>2</sub>O Nanocomposite for Photocatalytic Degradation of Naphthol Blue Black Dye, *Journal of Inorganic and Organometallic, Polym. Mater.* **28**, 540 (2018).
14. M. T. Makhlof, B. M.Abu-Zied, T. H. Mansoure, Effect of calcination on the H<sub>2</sub>O<sub>2</sub> decomposition activity of nano-crystalline CO<sub>3</sub>O<sub>4</sub> prepared by combustion method, *Appl. Surf. Sci.*, **274**, 45 (2013).
15. C. Y.Pan, Y.Yan, H. D.Li, S.Hu, Synthesis of bismuth oxide nanoparticles by a templating method and its photocatalytic performance, *Adv. Mater. Res.*, **557**, 615 (2012).
16. J. La, Y. Huang, G. Luo, J. Lai, C. Liu, G. Chu, Synthesis of bismuth oxide nanoparticles by solution combustion method, *Particu. Sci. Technol.*, **31**, 287 (2013).
17. G. Viruthagiri, P. Kannan, Visible light mediated photocatalytic activity of cobalt doped Bi<sub>2</sub>O<sub>3</sub> nanoparticles, *J Mater. Res. Technol.*, 127 (2017).
18. A. M.Abu-Dief, W. S. Mohamed,  $\alpha$ -Bi<sub>2</sub>O<sub>3</sub> nanorods: synthesis, characterization and UV-photocatalytic activity, *Mater. Res. Express*, **4**, 1 (2017).
19. M. Rivenet, P. Roussel, F. Abraham, One-dimensional inorganic arrangement in the bismuth oxalate hydroxide Bi (C<sub>2</sub>O<sub>4</sub>) OH, *J Solid State Chem.*, **181**, 2586 (2008).
20. L. L. Ding, Q. Zhao, J. L.Zhu, Z. J. Fan, B. Liu, The preparation and property Research of Bismuth oxide Nanospheres, In International Conference on Materials Chemistry and Environmental Protection 2015 Atlantis Press. (2016).
21. S. Ramachandran, A. Sivasamy, Synthesis of nanocrystalline bismuth oxide and its visible Photocatalytic activity in the degradation of an organic dye, *Inorg. Nano-Metal Chem.*, **48**, 225 (2018).
22. W. Raza, M. M. Haque, M. Muneer, T. Harada, M. Matsumura, Synthesis, characterization and photocatalytic performance of visible light induced bismuth oxide nanoparticles, *J Alloy Comp.*, **648**, 641 (2015).
23. S. K. Maji, N. Mukherjee, A. Mondal, B. Adhikary, Synthesis characterization and photo catalytic activity of  $\alpha$ -Fe<sub>2</sub>O<sub>3</sub> Nanoparticles, *Polyhedron*, **33**, 145 (2012).
24. C. Ren, B. Yang, M. Wu, J.Xu, Z. Fu, T.Guo, C.Zhu, Synthesis of Ag/ZnO nanorodes arrey with enhanced photocatalytic performance, *J Hazard. Meter.*, **182**, 123 (2010).
25. M. Selvapandiyan, K. Sathiyaraj, Synthesis, preparation, structural, optical, morphological and elemental analysis of bismuth oxides nanoparticles. *Silicon.*, **12**, 2309 (2020).
26. Y. Yan, Z. Zhou, Y. Cheng, Template-free fabrication of  $\alpha$ -and  $\beta$ -Bi<sub>2</sub>O<sub>3</sub> hollow spheres and their visible light photocatalytic activity for water purification. *J Alloys Compd.*, **605**, 102 (2014).
27. L. Xinjuan , P. Likun, L. Tian, S. Zhuo, Q. S. Chang Q. Sun, Visible light photocatalytic degradation of dyes by bismuth oxide-reduced graphene oxide composites prepared via microwave-assisted method, *J. Cool. Interface Sci.*, **408**, 145 (2013).
28. B. Viswanathan, Photocatalytic Degradation of Dyes: An Overview, *Curr. Catal.*, **7**, 99(2018).
29. X. Li, Y. Hou, Q. Zhao, L. Wang A general, one-step and template-free synthesis of sphere-like zinc ferrite nanostructures with enhanced photocatalytic activity for dye degradation, *J Colloi. Interf.ace Sci.*, **358**, 102(2011).
30. A. Elaziouti, B. Ahmed, ZnO-assisted photocatalytic degradation of Congo Red and Benzopurpurine 4B in aqueous solution, *J Chem. Eng. Proc. Technol.*, **2**, 1 (2011).
31. F. Zhang, J. Zhao, T. Shan, H. Hidaka,E., Pelizzetti,N.Serpone, TiO<sub>2</sub> assisted photo degradation of dye pollutants: II. Adsorption and degradation kinetics of eosin in TiO<sub>2</sub> dispersions under visible light irradiation, *Appl. Catal. B- Environ.*, **15**, 147 (1998).
32. U. G.Akpan,B. H. Hameed, Parameters affecting the photocatalytic degradation of dyes using TiO<sub>2</sub>-based photo catalysts: a review,*J Hazard. Mater.*, **170**,520(2009).
33. F. M. A. Aguirre, R H. Becerra, New synthesis of bismuth oxide nanoparticles Bi<sub>2</sub>O<sub>3</sub> assisted by tannic acid, *Appl. Physics, A* **119**, 909 (2015).
34. G. Mamba,M.A.Mamo, X.Y.Mbianda, A.K. Mishra, Nd, N, S-TiO<sub>2</sub> decorated onreducedgraphene oxide for a visible light active photocatalyst for dye degradation: Comparison to its MWCNT/Nd, N, S-TiO<sub>2</sub> analogue, *Indus. Eng. Chem. Res.*, **53**, 14329(2014).